



RESEARCH ARTICLE

10.1002/2014EF000244

Stratospheric ozone response to a solar irradiance reduction in a quadrupled CO₂ environmentCharles H. Jackman¹ and Eric L. Fleming^{1,2}¹NASA Goddard Space Flight Center, Greenbelt, Maryland, USA, ²Science Systems and Applications, Inc., Lanham, Maryland, USA

Key Points:

- Quadrupling CO₂ strongly perturbs the stratosphere
- Solar flux reduction in a quadrupled CO₂ atmosphere increases total column ozone
- Both quadrupled CO₂ and reduced solar flux cools the stratosphere and increases ozone

Corresponding author:

C. H. Jackman, Charles.H.Jackman@nasa.gov

Citation:

Jackman, C. H., and E. L. Fleming (2014), Stratospheric ozone response to a solar irradiance reduction in a quadrupled CO₂ environment, *Earth's Future*, 2, 331–340, doi:10.1002/2014EF000244.

Received 25 MAR 2014

Accepted 11 JUN 2014

Accepted article online 16 JUN 2014

Published online 10 JUL 2014

Abstract We used the Goddard Space Flight Center (GSFC) global two-dimensional (2D) atmospheric model to investigate the stratospheric ozone response to a proposed geoengineering activity wherein a reduced top-of-atmosphere (TOA) solar irradiance is imposed to help counteract a quadrupled CO₂ atmosphere. This study is similar to the Geoengineering Model Intercomparison Project (GeoMIP) Experiment G1. Three primary simulations were completed with the GSFC 2D model to examine this possibility: (A) a pre-industrial atmosphere with a boundary condition of 285 ppmv CO₂ (*piControl*); (B) a base future atmosphere with 1140 ppmv CO₂ (*abrupt4xCO2*); and (C) a perturbed future atmosphere with 1140 ppmv CO₂ and a 4% reduction in the TOA total solar irradiance (*G1*). We found huge ozone enhancements throughout most of the stratosphere (up to 40%) as a result of a large computed temperature decrease (up to 18 K) when CO₂ was quadrupled (compare simulation *abrupt4xCO2* to *piControl*). Further, we found that ozone will additionally increase (up to 5%) throughout most of the stratosphere with total ozone increases of 1–2.5% as a result of a reduction in TOA total solar irradiance (compare simulation *G1* to *abrupt4xCO2*). Decreases of atomic oxygen and temperature are the main drivers of this computed ozone enhancement from a reduction in TOA total solar irradiance.

1. Introduction

Several geoengineering activities have been proposed as possible techniques to help counteract the ongoing climate change caused by the increase in anthropogenic greenhouse gas emissions [e.g., *Kravitz et al.*, 2011]. Some geoengineering techniques involve carbon dioxide removal (CDR) while others involve solar radiation management (SRM). SRM techniques include reduction of solar radiation via stratospheric sulfate aerosols [e.g., *Crutzen*, 2006] and a space-based “sunshade” located at the Lagrange point (L1) between the Earth and the Sun [e.g., *Angel*, 2006]. The Geoengineering Model Intercomparison Project (GeoMIP) has coordinated an effort involving a large number of climate models to investigate the impact of possible techniques to help counteract environmental climate change. Two recent studies resulting from GeoMIP activities [*Schmidt et al.*, 2012; *Kravitz et al.*, 2013] investigated the impact of a reduction of the top-of-atmosphere (TOA) solar radiation on the Earth's climate in an enhanced CO₂ environment.

Kravitz et al. [2013] focused on Experiment G1 of GeoMIP, which requires a global surface radiative balance for the climate response to an abrupt quadrupling of CO₂ via a globally uniform reduction in TOA solar radiation. The 12 models participating in the *Kravitz et al.* [2013] investigation showed that reductions of TOA solar radiation in the range 3.5–5% were required to balance the dramatic CO₂ enhancement. These computed solar radiation reductions are in reasonable agreement with earlier studies [3.6% in *Govindasamy et al.*, 2003; 4.2% in *Lunt et al.*, 2008; and a range of 3.5–4.7% from the four models participating in *Schmidt et al.*, 2012]. Four papers [*Govindasamy et al.*, 2003; *Lunt et al.*, 2008; *Schmidt et al.*, 2012; *Kravitz et al.*, 2013] investigated various surface and tropospheric changes as a result of GeoMIP Experiment G1. As pointed out in *Schmidt et al.* [2012], some climate parameters were not addressed in these previous studies of G1. This included modifications to the stratosphere and mesosphere.

In this paper, we investigate the stratospheric ozone impacts of the solar reduction by approximating GeoMIP Experiment G1 with the use of a two-dimensional (2D) atmospheric model that has a comprehensive stratospheric and mesospheric chemistry representation (described in the following section). Specifically, we invoke a TOA solar radiation reduction in a quadrupled CO₂-modified atmosphere and investigate the impact on the stratosphere, primarily focusing on constituents and temperature.

This is an open access article under the terms of the Creative Commons Attribution-NonCommercial-NoDerivs License, which permits use and distribution in any medium, provided the original work is properly cited, the use is non-commercial and no modifications or adaptations are made.

GeoMIP Experiment G1 requires a balance of the forcing at the Earth's surface from CO₂ within ± 0.1 W/m² [e.g., see Schmidt *et al.*, 2012; Kravitz *et al.*, 2013]. However in the present study, we approximate G1 via forcing a TOA solar radiation reduction of 4%, which is in the range of the previous GCM studies cited above.

This paper contains four primary sections, including the introduction. The 2D chemistry-climate model is discussed in section 2. The model simulations and results are discussed in section 3 and the conclusions are given in section 4.

2. Model Description

The latest version of the Goddard Space Flight Center (GSFC) 2D (latitude vs. altitude) atmospheric model was used to predict the stratospheric ozone effects of a TOA reduction of 4% in total solar irradiance (TSI) following a quadrupling of the CO₂ concentration. This model was first discussed over 20 years ago [Douglass *et al.*, 1989; Jackman *et al.*, 1990], and the coupled chemistry-radiation-dynamics version of the model used in the present study was originally discussed in Bacmeister *et al.* [1995]. The model has been applied to chemistry-climate coupling studies of the middle atmosphere (stratosphere and mesosphere), and has undergone extensive improvements over the years [e.g., Considine *et al.*, 1994; Jackman *et al.*, 1996; Rosenfield *et al.*, 1997, 2002; Fleming *et al.*, 1999, 2007, 2011]. These recent studies have shown that the residual circulation framework used in the 2D model provides realistic simulations of stratospheric transport on long timescales (>30 days), as the model simulations show good overall agreement with a variety of observations in reproducing transport-sensitive features in the meridional plane. The model uses a chemical solver described in Jackman *et al.* [2005] and Fleming *et al.* [2007, 2011]. The photochemical gas and heterogeneous reaction rates and photolysis cross sections are from the latest Jet Propulsion Laboratory recommendations [Sander *et al.*, 2010]. The vertical range of the model, equally spaced in log pressure, is from the ground to approximately 92 km (0.0024 hPa), with ~ 1 km grid spacing; the latitude grid spacing is 4°.

Some of the 2D model components are very similar to the Goddard Earth Observing System 3D chemistry-climate model (GEOSCCM). The GEOSCCM couples the GEOS-5 general circulation model with stratospheric chemistry [e.g., Stolarski *et al.*, 2006; Pawson *et al.*, 2008; Newman *et al.*, 2009] and has been evaluated in CCM intercomparisons [e.g., Eyring *et al.*, 2006, 2007, 2010]. The common model components include the infrared (IR) radiative transfer scheme [Chou *et al.*, 2001]; the photolytic calculations [Anderson and Lloyd, 1990; Jackman *et al.*, 1996]; and the microphysical model from polar stratospheric cloud (PSC) formation [Considine *et al.*, 1994]. Also, the 2D model accounts for CO₂-induced changes in surface temperature (including sea surface temperature), latent heating, and tropospheric water vapor by parameterizing these quantities using the CO₂ ground boundary condition and sensitivity factors derived from the GEOSCCM simulations [Oman *et al.*, 2010]. The resulting CO₂-induced tropospheric warming, stratospheric cooling, and acceleration of the stratospheric Brewer-Dobson circulation (BDC) in the 2D model were shown to be very similar to the GEOSCCM [Fleming *et al.*, 2011], as was the response to solar flux perturbations [Swartz *et al.*, 2012]. Therefore, we expect the 2D and GEOSCCM models to give very similar stratospheric responses to the CO₂ and solar flux perturbations addressed in this paper. Oman *et al.* [2010] relies on the AR4 integrations of the National Center for Atmospheric Research (NCAR) Community Climate System Model, Version 3 for sea surface temperatures in future GEOSCCM simulations. Neither the GEOSCCM nor the 2D model can be used to predict surface temperature changes caused by a reduction in TOA solar radiation.

3. Model Simulations and Results

For this study, 30-year steady state primary simulations were made for (1) the pre-industrial atmosphere (*piControl*), (2) CO₂ quadrupled from the pre-industrial atmosphere (*abrupt4xCO2*), and (3) CO₂ quadrupled plus a 4% reduction in TOA solar flux at all wavelengths which approximates GeoMIP Experiment G1 (*G1*). The primary simulations are summarized in Table 1. We also completed four other 30-year steady state sensitivity simulations: (4) the pre-industrial atmosphere with a 4% reduction in TOA solar flux (*piControlG1*), (5) CO₂ quadrupled plus a 4% reduction in TOA solar flux at wavelengths <242 nm (*G1 < 242nm*), (6) CO₂ quadrupled but with the temperature fixed (*abrupt4xCO2ft*), and (7) CO₂ quadrupled plus a 4%

Table 1. Description of GSFC 2D Primary Simulations

Simulation Designation	CO ₂ Ground Boundary Condition	Solar Flux Reduction	Wavelengths Affected
<i>piControl</i>	285 ppmv	No	-
<i>abrupt4xCO2</i>	1140 ppmv	No	-
<i>G1</i>	1140 ppmv	Yes	All (−4%)

Table 2. Description of GSFC 2D Sensitivity Simulations

Simulation Designation	CO ₂ Ground Boundary Condition	Solar Flux Reduction	Wavelengths Affected	Other Information
<i>piG1</i>	285 ppmv	Yes	All (−4%)	-
<i>G1 < 242nm</i>	1140 ppmv	Yes	<242 nm (−4%)	-
<i>abrupt4xCO2ft</i>	1140 ppmv	No	-	Fixed Temperature
<i>G1ft</i>	1140 ppmv	Yes	All (−4%)	Fixed Temperature

reduction in TOA solar flux at all wavelengths, but with the temperature fixed (*G1ft*). These sensitivity simulations are summarized in Table 2. Unlike 3D CCMs, the 2D model has negligible interannual variability. The model's steady state prediction of atmospheric composition is in a seasonally repeating condition wherein the composition changes daily but repeats annually [e.g., see *Jackman et al.*, 1998]. The results presented in this paper are from the final year of the steady state simulations.

The *piControl* ground boundary conditions are set at 1850 values for the GHGs [*Hansen and Sato*, 2004]: 285 parts per million by volume (ppmv) for CO₂, and 275 parts per billion by volume (ppbv) and 790 ppbv for N₂O and CH₄, respectively. Anthropogenically produced CFCs and halons are set to zero. Naturally occurring CH₃Cl and CH₃Br are set to 440 parts per trillion by volume (pptv) and 5 pptv, respectively [*Butler et al.*, 1999]. For the quadrupled CO₂ atmosphere (*abrupt4xCO2*), the ground boundary condition for CO₂ is set to 1140 ppmv, with all other gases set to the *piControl* conditions (see Table 1).

Quadrupling CO₂ in the atmosphere and holding the solar constant fixed (compare simulation *abrupt4xCO2* to simulation *piControl*) results in substantial cooling throughout the stratosphere and lower mesosphere (100–0.1 hPa), as shown in Figure 1 (top left). The largest cooling (~17–18 K) occurs near the polar stratopause (~1 hPa). This computed upper stratospheric cooling is similar to that predicted by *Govindasamy et al.* [2003] using Version 3 of the Community Climate Model (CCM3) for a quadrupled CO₂ scenario.

The predicted reductions in temperature (T) above 100 hPa caused ozone increases throughout most of the stratosphere and lower mesosphere (see Figure 1, top right). These results were not surprising since such ozone enhancements caused by CO₂-induced stratospheric cooling have been computed before [e.g., *Haigh and Pyle*, 1979; *Rosenfield et al.*, 2002; *Shepherd and Jonsson*, 2008; *Li et al.*, 2009; *Fleming et al.*, 2011]. The largest ozone enhancements (30–40%) in Figure 1 are predicted in the upper stratosphere (1–5 hPa). Many of the reaction rates involved in ozone destruction are highly temperature dependent, with lower temperatures resulting in slower loss rates [e.g., $k = 8 \times 10^{-12} \exp(-2060/T)$ is the reaction rate for $O + O_3 \rightarrow O_2 + O_2$, a key reaction governing ozone loss]. Since the rate determining steps of the other ozone loss cycles have only modest temperature dependences, the T decreases drive most of the ozone increases [also, see *Rosenfield et al.*, 2002].

The predicted decreases in ozone in the lower tropical stratosphere (~20–100 hPa, ~40°S–50°N, see Figure 1, top right) are mainly due to the acceleration of the BDC caused by the CO₂ increases, and are common features among CCMs [e.g., *Garcia and Randel*, 2008; *Li et al.*, 2009; *Fleming et al.*, 2011; *World Meteorological Organization (WMO)*, 2011]. The enhanced tropical upwelling of the accelerated BDC advects ozone-poor air upwards from the tropical troposphere. The corresponding descending branch of the BDC advects ozone-rich air downwards from the middle stratosphere in the extratropics, leading to ozone increases in the lower stratosphere at mid-high latitudes [*Li et al.*, 2009]. The tropical lower

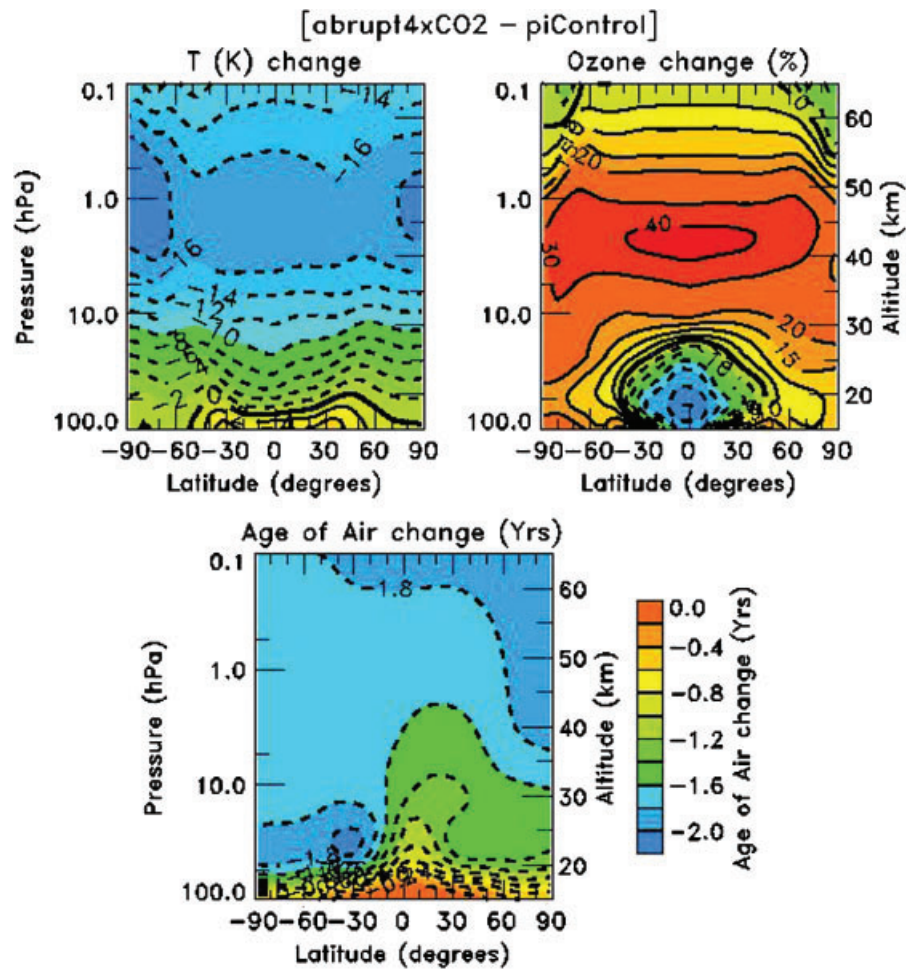


Figure 1. Annual average computed Temperature (K) (top left), ozone (%) (top right), and age-of-air (years) change (bottom) from GSFC 2D model simulation *piControl* to *abrupt4xCO2* (see Table 1). Contour intervals for Temperature and age-of-air are 2 K and 0.2 years, respectively. Contour levels for ozone change are -50, -40, -30, -20, -15, -10, -5, 0, 5, 10, 15, 20, 30, and 40%.

stratospheric ozone decreases in Figure 1 (top right) are also likely caused in part by the “self-destruction” of ozone, whereby enhancements in upper stratospheric ozone allow less ozone-producing ultraviolet (UV) light to penetrate to lower altitudes. This process is basically the inverse of ozone self-healing, wherein ozone decreases in the middle and upper stratosphere lead to ozone enhancements in the lower stratosphere. Ozone self-healing has been discussed in some detail in the literature [e.g., *Mills et al.*, 2008].

Stratospheric water vapor increases by 20–30% between simulation *piControl* and *abrupt4xCO2*. These changes are primarily driven by the use of GEOSCCM tropospheric water vapor values in the 2D model (see discussion in section 2).

The resulting changes in total column ozone are shown in Figure 2. Large increases greater than 10% are predicted at middle and high latitudes (>40°) in both hemispheres when CO₂ is quadrupled. More modest total ozone increases (<10%) are computed at lower latitudes (15°–40°) in both hemispheres. Near the equator, small decreases (up to ~3%) are predicted in the total column, as the ozone reductions in the lower stratosphere outweigh the ozone increases in the middle and upper stratosphere seen in Figure 1 (top right). The annually averaged global total ozone (AAGTO) is computed to increase by 6.8% between simulations *piControl* and *abrupt4xCO2* (see Table 3).

Acceleration of the BDC in an increasing CO₂ environment also leads to a reduction in the stratospheric age-of-air computed in CCMs, as discussed in previous studies [e.g., *Austin and Li*, 2006; *Garcia and Randel*, 2008; *Oman et al.*, 2009]; the 2D model age-of-air change through the 21st century using the IPCC A1B scenario [*Intergovernmental Panel on Climate Change (IPCC)*, 2000] was shown to be very similar to the

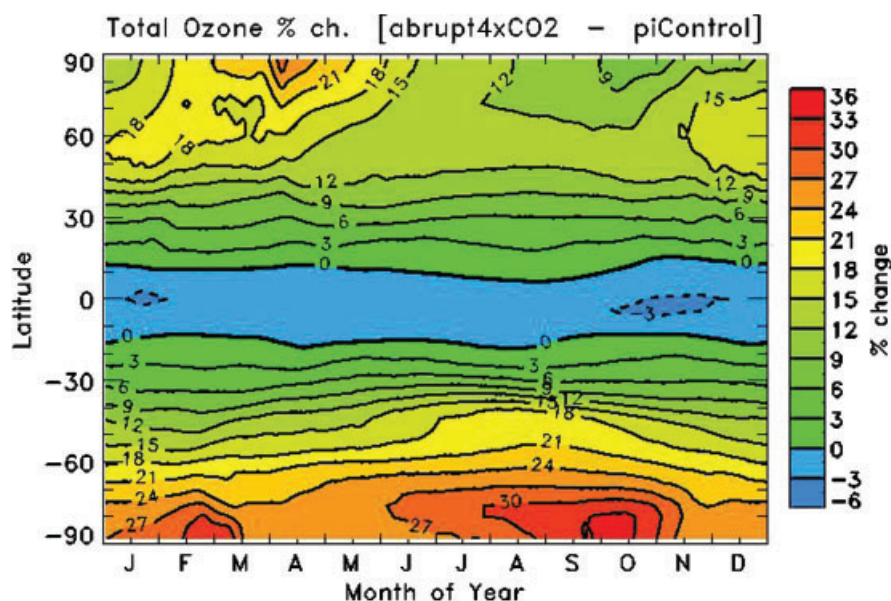


Figure 2. Computed total column ozone (%) change from GSFC 2D model simulation *piControl* to *abrupt4xCO2* (see Table 1) as a function of month and latitude. Contour intervals are 3%.

Table 3. Annually Averaged Global Total Ozone (AAGTO) Comparisons

Simulations Differenced	AAGTO Change (%)
<i>abrupt4xCO2</i> - <i>piControl</i>	6.8
<i>G1</i> - <i>abrupt4xCO2</i>	1.6
<i>G1 < 242nm</i> - <i>abrupt4xCO2</i>	-0.2
<i>G1ft</i> - <i>abrupt4xCO2ft</i>	1.1
<i>piG1</i> - <i>piControl</i>	1.8

GEOSCCM [Fleming et al., 2011]. For the *abrupt4xCO2* simulation, the 2D model age-of-air change from the *piControl* simulation due to the quadrupling of CO₂ is shown in Figure 1 (bottom). Age-of-air is decreased significantly throughout the stratosphere, with maximum reductions of 1.4–2 years in the upper stratosphere globally and in the SH extratropical lower stratosphere. This represents a change of 30–40% in these regions where the age-of-air in the *piControl* simulation is computed to be a maximum of 5–6 years.

GeoMIP Experiment G1 involves a comparison of two simulations with a quadrupled CO₂: (1) base solar flux (*abrupt4xCO2*), and (2) a 4% reduction in TSI (*G1*). The ozone, O^{(3)P}, HO_x (H + OH + HO₂), and Temperature changes from simulation *abrupt4xCO2* to simulation *G1* are given in Figure 3. Ozone (Figure 3, top left) is enhanced throughout most of the stratosphere and lower mesosphere as a result of a 4% reduction in TSI. Large ozone increases are predicted to be >5% from ~2 to 0.7 hPa between 60°S and 60°N latitude. There is also a region of decreased ozone in the tropical lower stratosphere (~20–100 hPa), which is primarily caused by the ozone “self-destruction” mechanism discussed above. This feature is likely not caused by changes in the BDC, since the lower tropical stratospheric upwelling changes between simulations *abrupt4xCO2* and *G1* are extremely small. Total ozone (Figure 4) is predicted to increase at all latitudes over the course of the year with enhancements of 1–1.5% in the tropics and 2–2.5% at polar latitudes. The AAGTO is computed to increase by 1.6% between *abrupt4xCO2* and *G1* (see Table 3).

Previous studies have generally shown that there is a positive correlation between solar flux perturbations (e.g., the 11-year solar cycle and 27-day solar rotation) and the corresponding stratospheric ozone response [e.g., WMO, 2007, 2011; Swartz et al., 2012; and references therein]. This is primarily due to the enhanced photolysis of O₂ and subsequent production of ozone with increased solar flux at wavelengths <242 nm. To explore this relationship in the present study, simulation *G1 < 242nm* reduces the TOA solar

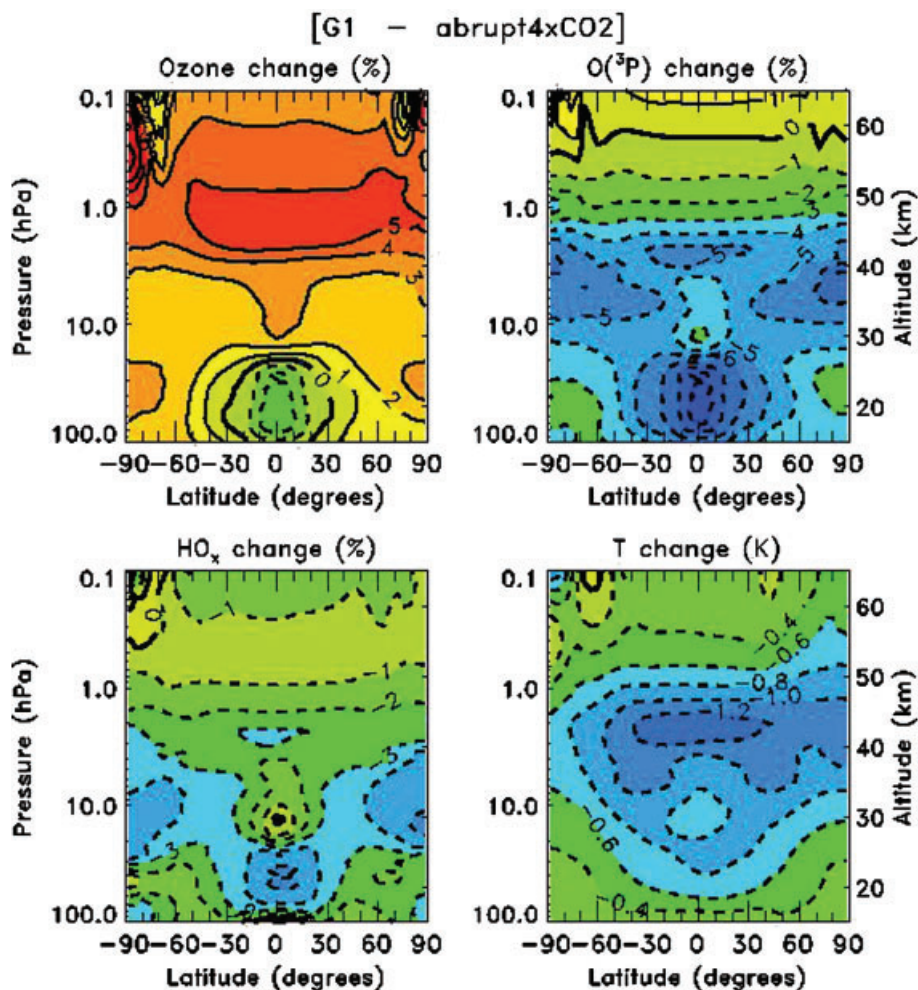
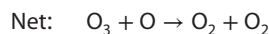


Figure 3. Annual average computed ozone (%) (top left), ground state atomic oxygen, O(³P), (%) (top right), HO_x (%) (bottom left), and Temperature (K) (bottom right) change from GSFC 2D model simulation *abrupt4xCO2* to *G1*. The *G1* simulation has the total solar irradiance reduced by 4% (see Table 1). Contour intervals for ozone, O(³P), and HO_x are 1%. Contour intervals for Temperature are 0.2K.

flux by 4% only at wavelengths < 242 nm (Table 2). The resulting AAGTO is computed to decrease by 0.2% from *abrupt4xCO2* to *G1* < 242nm (see Table 3). Given this correlation between solar shorter wavelength UV flux decrease and ozone decrease, it was somewhat surprising to compute an ozone increase (Figures 3 and 4) caused by a 4% reduction in the solar flux at all wavelengths (i.e., TSI). We next focus on various photochemical components from the GSFC 2D model to help explain these results.

When solar flux is reduced at all wavelengths, atomic oxygen, both ground state [O(³P)] and excited state [O(¹D)], is decreased throughout most of the 100–0.1 hPa region due primarily to the reduction in ozone photolysis ($O_3 + h\nu (<1100 \text{ nm}) \rightarrow O_2 + O$). Stratospheric O(³P) is computed to decrease by 2–7% (see Figure 3, top right), with similar reductions computed for O(¹D).

Many of the catalytic cycles controlling ozone and odd oxygen ($O_x = O_3 + O$, which is >99% ozone in the stratosphere and lower mesosphere), are two step processes, wherein the second reaction involving ground state atomic oxygen, O(³P), is called the “rate-limiting” step. Consider the HO_x reaction sequence, which results in the destruction of odd oxygen (O_x):



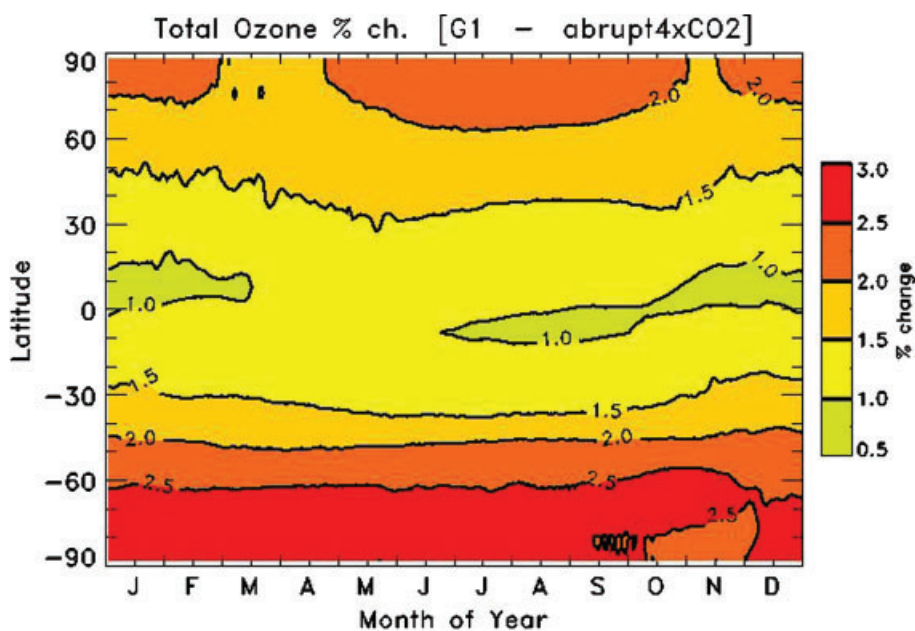
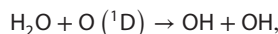


Figure 4. Computed total column ozone (%) change from GSFC 2D model simulation *abrupt4xCO2* to *G1* as a function of month and latitude. The *G1* simulation has the total solar irradiance reduced by 4% (see Table 1).

Throughout most of the stratosphere, reaction (2) is the slower, or “rate-limiting,” step in this HO_x loss process. The speed of this O_x loss process in much of the stratosphere is ultimately dependent on the concentration of O , thus a reduction in O will result in an increase in ozone. Adding to the ozone enhancement is the fact that the abundance of reactive HO_x constituents H , OH , and HO_2 has been reduced because of the decrease in the atomic oxygen excited state, $\text{O}(^1\text{D})$. The main reaction generating HO_x



does not proceed as rapidly. Also, stratospheric H_2O is slightly reduced (up to -0.55%) primarily due to decreases in the stratospheric oxidation of CH_4 [reaction with OH or $\text{O}(^1\text{D})$] from the 4% reduction in TSI.

HO_x constituents are predicted to decrease by 1–6% in the stratosphere (see Figure 3, bottom left). Less OH and HO_2 molecules ultimately mean that the catalytic cycle to destroy ozone represented by reactions (1) and (2) is slower and ozone will be increased with the reduction in TSI.

As a caveat, we need to add that not all reactive constituents are decreased throughout the stratosphere in the reduced TSI environment. Some NO_x , ClO_x , and BrO_x constituents responsible for ozone loss are modestly enhanced (up to 5%) at some levels (primarily at pressures <10 hPa) due to slight increases in the source gases responsible for their production. Although the surface boundary conditions for the source gases do not change, slight increases in the atmospheric concentrations of the source gases N_2O , CH_3Cl , and CH_3Br are caused by reduced photolysis and $\text{O}(^1\text{D})$ loss as a result of the 4% reduction in TSI. However, the computed total O_x photochemical loss is reduced throughout the 100–0.1 hPa range, thus there is a general ozone enhancement.

To reiterate: the primary factor contributing to the stratospheric ozone increase is the reduction in atomic oxygen (both $\text{O}(^3\text{P})$ and $\text{O}(^1\text{D})$). Another factor contributing to this stratospheric ozone increase is the positive feedback effect caused by the associated temperature changes. The TSI decrease reduces the rate of ozone photolysis, which is the main source of heating in the stratosphere, and therefore causes a small cooling throughout the stratosphere (see Figure 3, bottom right). The computed temperature reductions are largest in the tropical upper stratosphere (1–1.2 K). As stated before, many of the reaction rates involved in odd oxygen destruction are highly temperature dependent (lower temperatures cause less ozone destruction), thus these T decreases also add to the computed ozone increase.

To investigate the significance of the temperature changes on our results, we ran two additional simulations with temperature not coupled to the chemistry changes (i.e., fixed temperature simulations: *abrupt4xCO2ft* and *G1ft*). Both simulations use the same set of specified temperatures which change daily and repeat yearly. We found that AAGTO increased by 1.1% from *abrupt4xCO2ft* to *G1ft* (see Table 3). Thus, the computed temperature change from *abrupt4xCO2* to *G1* was responsible for about one-third of the increase in AAGTO.

To investigate the impact of the background atmosphere on our results, we ran an additional sensitivity simulation with the TOA TSI reduced by 4% in the pre-industrial atmosphere (*piG1*). We found that the AAGTO increased by 1.8% from *piControl* to *piG1* (see Table 3). Thus, this somewhat different background atmosphere with higher stratospheric temperatures (see Figure 1) resulted in a slightly larger ozone increase when the TOA TSI was reduced, compared to imposing the TOA TSI reduction on the quadrupled CO₂ atmosphere.

The total column ozone increase (see Figure 4) from the 4% TSI decrease is predicted to lead to an additional solar UVB flux decrease at the Earth's surface. The magnitude of this change is dependent on latitude and season. For example at tropical latitudes, the annually averaged UVB flux in wavelengths 280–315 nm at the Earth's surface is computed to decline between 12% (280 nm) and 4.4% (315 nm). Most of the change in the 315–350 nm band in the tropics is due to the 4% TSI decrease, however, larger changes are computed at higher latitudes due to the stratospheric ozone enhancements. The solar flux at wavelengths >350 nm is primarily influenced by the 4% TSI decrease and not significantly by the overhead ozone change, thus is reduced by about 4% at the Earth's tropical surface.

4. Conclusions

We used the GSFC 2D atmospheric model to investigate the stratospheric response to a proposed geo-engineering activity wherein a reduced TOA TSI is imposed to help counteract a quadrupled CO₂ atmosphere. We found huge ozone enhancements throughout most of the stratosphere (up to 40%) as a result of a large computed temperature decrease (up to 18 K) when CO₂ was quadrupled from 285 to 1140 ppmv. Total ozone increased outside the equatorial region (>±15°) in both hemispheres when CO₂ was quadrupled. We found that a 4% reduction in the TSI at the TOA results in an additional ozone increase throughout most of the stratosphere in this quadrupled CO₂ atmosphere. Total column ozone was computed to increase by 1–2.5% as a result of this 4% reduction in TSI at the TOA. A reduction in atomic oxygen and temperature are the main drivers of these computed ozone enhancements. Thus, both a quadrupled CO₂ atmosphere as well as an atmosphere with a 4% reduction in TSI at the TOA result in computed enhancements in total column ozone outside of the tropics (>±15°).

Although the 4% reduction was selected because it is within the range of earlier GCM studies (3.5–5%), the exact solar reduction imposed will slightly change the quantitative results, but not the overall conclusions, of the paper. Other previous studies of GeoMIP Experiment G1 with fully coupled atmosphere-ocean-general circulation models investigated latitudinal surface temperature differences, Arctic sea ice loss, precipitation and convection changes, and plant productivity changes [Govindasamy *et al.*, 2003; Lunt *et al.*, 2008; Schmidt *et al.*, 2012; Kravitz *et al.*, 2013]. As indicated in section 2, the 2D model used in this study does not predict solar flux-induced surface temperature changes, thus the inclusion of ozone photochemistry in future fully coupled GCM simulations of GeoMIP Experiment G1 is recommended to investigate possible stratospheric feedbacks on the troposphere.

Acknowledgments

We thank the NASA Headquarters Atmospheric Composition Modeling and Analysis Program for support during the time that this manuscript was written. We thank Valentina Aquila and Paul Newman for valuable comments on an earlier version of this paper. The GSFC 2D Model output used in this manuscript will be provided to interested individuals upon request to author C. Jackman (Charles.H.Jackman@nasa.gov).

References

- Anderson, D. E., and S. A. Lloyd (1990), Polar twilight UV-visible radiation field: perturbations due to multiple scattering, ozone depletion, stratospheric clouds, and surface albedo, *J. Geophys. Res.*, *95*, 7429–7434, doi:10.1029/JD095iD06p07429.
- Angel, R. (2006), Feasibility of cooling the Earth with a cloud of small spacecraft near the inner Lagrange point (L1), *Proc. Natl. Acad. Sci. U. S. A.*, *103*, 17,184–17,189.
- Austin, J., and F. Li (2006), On the relationship between the strength of the Brewer-Dobson circulation and the age of stratospheric air, *Geophys. Res. Lett.*, *33*, L17807, doi:10.1029/2006GL026867.
- Bacmeister, J. T., M. R. Schoeberl, M. E. Summers, J. R. Rosenfield, and X. Zhu (1995), Descent of long-lived trace gases in the winter polar vortex, *J. Geophys. Res.*, *100*, 11669–11684, doi:10.1029/94JD02958.
- Butler, J. H., M. Battle, M. L. Bender, S. A. Montzka, A. D. Clarke, E. S. Saltzman, C. M. Sucher, J. P. Severinghaus, and J. W. Elkins (1999), A record of atmospheric halocarbons during the twentieth century from polar firn air, *Nature*, *399*, 749–755.

- Chou, M.-D., M. J. Suarez, X.-Z. Liang, and M.-H. Yan (2001), A thermal infrared radiation parameterization for atmospheric studies, NASA Tech. Memo. NASA/TM-2001-104606, 9, 56 pp., Greenbelt, Md.
- Considine, D. B., A. R. Douglass, and C. H. Jackman (1994), Effects of a polar stratospheric cloud parameterization on ozone depletion due to stratospheric aircraft in a two-dimensional model, *J. Geophys. Res.*, *99*, 18,879–18,894, doi:10.1029/94JD01026.
- Crutzen, P. J. (2006), Albedo enhancement by stratospheric sulphur injections: A contribution to resolve a policy dilemma?, *Clim. Change*, *77*, 211–219.
- Douglass, A. R., C. H. Jackman, and R. S. Stolarski (1989), Comparison of model results transporting the odd nitrogen family with results transporting separate odd nitrogen species, *J. Geophys. Res.*, *94*, 9862–9872, doi:10.1029/JD094iD07p09862.
- Eyring, V., et al. (2006), Assessment of temperature, trace species, and ozone in chemistry-climate model simulations of the recent past, *J. Geophys. Res.*, *111*, D22308, doi:10.1029/2006JD007327.
- Eyring, V., et al. (2007), Multimodel projections of stratospheric ozone in the 21st century, *J. Geophys. Res.*, *112*, D16303, doi:10.1029/2006JD008332.
- Eyring, V., et al. (2010), Multi-model assessment of stratospheric ozone return dates and ozone recovery in CCMVal-2 models, *Atmos. Chem. Phys.*, *10*, 9451–9472, doi:10.5194/acp-10-9451-2010.
- Fleming, E. L., C. H. Jackman, D. B. Considine, and R. S. Stolarski (1999), Simulation of stratospheric tracers using an improved empirically based two-dimensional model transport formulation, *J. Geophys. Res.*, *104*, 23911–23934, doi:10.1029/1999JD00332.
- Fleming, E. L., C. H. Jackman, D. K. Weisenstein, and M. K. W. Ko (2007), The impact of inter-annual variability on multidecadal total ozone simulations, *J. Geophys. Res.*, *112*, D10310, doi:10.1029/2006JD007953.
- Fleming, E. L., C. H. Jackman, R. S. Stolarski, and A. R. Douglass (2011), A model study of the impact of source gas changes on the stratosphere for 1850–2100, *Atmos. Chem. Phys.*, *11*, 8515–8541.
- Garcia, R. R., and W. J. Randel (2008), Acceleration of the Brewer-Dobson circulation due to increases in greenhouse gases, *J. Atmos. Sci.*, *65*, 2731–2739.
- Govindasamy, B., K. Caldeira, and P. B. Duffy (2003), Geoengineering Earth's radiation balance to mitigate climate change from a quadrupling of CO₂, *Global Planet. Change*, *37*, 157–168.
- Haigh, J. D., and J. A. Pyle (1979), A two-dimensional calculation including atmospheric carbon dioxide and stratospheric ozone, *Nature*, *279*(222–224), 1979.
- Hansen, J., and M. Sato (2004), Greenhouse gas growth rates, *Proc. Natl. Acad. Sci. U. S. A.*, *101*(46), 16109–16114.
- Intergovernmental Panel on Climate Change (IPCC) (2000), *Special Report on Emissions Scenarios: A Special Report of Working Group III of the Intergovernmental Panel on Climate Change*, 599 pp, Cambridge Univ. Press, Cambridge, UK.
- Jackman, C. H., A. R. Douglass, R. B. Rood, R. D. McPeters, and P. E. Meade (1990), Effect of solar proton events on the middle atmosphere during the past two solar cycles as computed using a two-dimensional model, *J. Geophys. Res.*, *95*, 7417–7428, doi:10.1029/JD095iD06p07417.
- Jackman, C. H., E. L. Fleming, S. Chandra, D. B. Considine, and J. E. Rosenfield (1996), Past, present, and future modeled ozone trends with comparisons to observed trends, *J. Geophys. Res.*, *101*, 28753–28767, doi:10.1029/96JD03088.
- Jackman, C. H., D. B. Considine, and E. L. Fleming (1998), A global modeling study of solid rocket aluminum oxide emission effects on stratospheric ozone, *Geophys. Res. Lett.*, *25*, 907–910, doi:10.1029/98GL00403.
- Jackman, C. H., M. T. DeLand, G. J. Labow, E. L. Fleming, D. K. Weisenstein, M. K. W. Ko, M. Sinnhuber, and J. M. Russell (2005), Neutral atmospheric influences of the solar proton events in October–November 2003, *J. Geophys. Res.*, *100*, A09S27, doi:10.1029/2004JA010888.
- Kravitz, B., A. Robock, O. Boucher, H. Schmidt, K. E. Taylor, G. Stenchikov, and M. Schulz (2011), The geoengineering model intercomparison project (GeoMIP), *Atmos. Sci. Lett.*, *12*, 162–167, doi:10.1002/asl.316.
- Kravitz, B., et al. (2013), Climate model response from the Geoengineering Model Intercomparison Project (GeoMIP), *J. Geophys. Res.*, *118*, doi:10.1002/jgrd.50646.
- Li, F., R. S. Stolarski, and P. A. Newman (2009), Stratospheric ozone in the post-CFC era, *Atmos. Chem. Phys.*, *9*, 2207–2213, doi:10.5194/acp-9-2207-2009.
- Lunt, D. J., A. Ridgwell, P. J. Valdes, and A. Seale (2008), “Sunshade World”: A fully coupled GCM evaluation of the climatic impacts of geoengineering, *Geophys. Res. Lett.*, *35*, L12710, doi:10.1029/2008GL033674.
- Mills, M. J., O. B. Toon, R. P. Turco, D. E. Kinnison, and R. R. Garcia (2008), Massive global ozone loss predicted following regional nuclear conflict, *Proc. Natl. Acad. Sci.*, *105*, 5307–5312.
- Newman, P. A., et al. (2009), What would have happened in the ozone layer if chlorofluorocarbons (CFCs) had not be regulated?, *Atmos. Chem. Phys.*, *9*, 2113–2128, doi:10.5194/acp-9-2113-2009.
- Oman, L. D., D. W. Waugh, S. Pawson, R. S. Stolarski, and P. A. Newman (2009), On the influence of anthropogenic forcings on changes in the stratospheric mean age, *J. Geophys. Res.*, *114*, D03105, doi:10.1029/2008JD010378.
- Oman, L. D., D. W. Waugh, S. R. Kawa, R. S. Stolarski, A. R. Douglass, and P. A. Newman (2010), Mechanisms and feedback causing changes in upper stratospheric ozone in the 21st century, *J. Geophys. Res.*, *115*, D05303, doi:10.1029/2009JD012397.
- Pawson, S., R. S. Stolarski, A. R. Douglass, P. A. Newman, J. E. Nielsen, S. M. Frith, and M. L. Gupta (2008), Goddard earth observing system chemistry-climate model simulations of stratospheric ozone-temperature coupling between 1950 and 2005, *J. Geophys. Res.*, *113*, D12103, doi:10.1029/2007JD009511.
- Rosenfield, J. E., D. B. Considine, P. E. Meade, J. T. Bacmeister, C. H. Jackman, and M. R. Schoeberl (1997), Stratospheric effects of Mount Pinatubo aerosol studied with a coupled two-dimensional model, *J. Geophys. Res.*, *102*, 3649–3670, doi:10.1029/96JD03820.
- Rosenfield, J. E., A. R. Douglass, and D. B. Considine (2002), The impact of increasing carbon dioxide on ozone recovery, *J. Geophys. Res.*, *107*, 4049, doi:10.1029/2001JD000824.
- Sander, S. P., et al. (2010), Chemical kinetics and photochemical data for use in atmospheric studies, Evaluation Number 17, *JPL Publication 10-6*.
- Schmidt, H., et al. (2012), Solar irradiance reduction to counteract radiative forcing from a quadrupling of CO₂: climate responses simulated by four Earth system models, *Earth Syst. Dyn.*, *3*, 63–78, doi:10.5194/esd-3-63-2012.
- Shepherd, T. G., and A. I. Jonsson (2008), On the attribution of stratospheric ozone and temperature changes to changes in ozonedepleting substances and well-mixed greenhouse gases, *Atmos. Chem. Phys.*, *8*, 1435–1444, doi:10.5194/acp-8-1435-2008.
- Stolarski, R. S., A. R. Douglass, M. Gupta, P. A. Newman, S. Pawson, M. R. Schoeberl, and J. E. Nielsen (2006), An ozone increase in the Antarctic summer stratosphere: a dynamical response to the ozone hole, *Geophys. Res. Lett.*, *33*, L21805, doi:10.1029/2006GL026820.

- Swartz, W. H., R. S. Stolarski, L. D. Oman, E. L. Fleming, and C. H. Jackman (2012), Middle atmosphere response to different descriptions of the 11-yr solar cycle in spectral irradiance in a chemistry-climate model, *Atmos. Chem. Phys.*, *12*, 5937–5948, doi:10.5194/acp-12-5937-2012.
- World Meteorological Organization (WMO) (2007), *Scientific Assessment of Ozone Depletion: 2006, Global Ozone Research and Monitoring Project-Rep. 50*, Geneva, Switzerland.
- World Meteorological Organization (WMO) (2011), *Scientific Assessment of Ozone Depletion: 2010, Global Ozone Research and Monitoring Project-Rep. 52*, Geneva, Switzerland.